Full Configuration Interaction Model for 1-D Quantum System

Adam Asaad

Department of Physics, Lund University

Bachelor Thesis (15 hp)

Supervised by Andrea Idini

September, 2021

LUND
UNIVERSITY

Abstract

The many-body problem is one of the most challenging problems in physics due to the complexity emerging from the interactions of many quantum particles. Since the advent of computers with increasing power, computational methods have been very successful in providing insight and precise solutions to this problem. We give an introduction to two canonically used methods, density functional theory and configuration interaction, providing the example of a valence space nuclear shell model calculation. In this work, we developed a program that applies the full configuration interaction method to a general 1-D quantum system with success, providing insight into the dynamics of a many-body system in different conditions of potential, interaction and number of particles.

Popular Abstract

One of the hardest problems in physics is figuring out what happens when you put a bunch of interacting sub-atomic particles together, this is called the many-body problem. This is important since many natural phenomena, everything from batteries to the burning of our sun, is caused by bundles of sub-atomic particles, usually in the form of atoms or atomic nuclei. The difficulty of the many-body problem comes from the fact that each particle's motion is affected by that of every other particle, making the equations that describe them very complicated and in most cases, impossible to solve by hand. This is where the relatively recent advent of computers has found use in tackling this problem numerically, using computational methods that have been developed specifically to take advantage of the ever increasing power of computers to find approximated and brute-force solutions for many types of these bundles, and with great success. In this manuscript, we give an introduction to some of these methods and demonstrate a computer program that applies them to a small collection of particles, such as a small nucleus.

Acknowledgements

Thanks to my family and friends for their support, and thanks to my supervisor for his patience.

Contents

List of Acronyms

DFT Density Functional Theory

CI Configuration Interaction

SD Slater Determinant

1 Introduction

The many-body problem is one of the most challenging and computationally intensive problem in physics. This is due to interacting particles coupling their equations of motion. This requires them to be solved simultaneously rather than be built up from independant solutions for each particle, which exponentially increases the complexity of the solution and resists analytical approach. The study of many-particle quantum systems is important for understanding many structures and processes in chemistry, solid-state physics, nuclear physics and by extension its application in astrophysical phenomena. In nuclear astrophysics, environments usually involve conditions that are not accessible experimentally, so describing different nuclear processes that occur in events like supernovae requires theoretical and computational means [1].

A significant example of this is the description of the nucleosynthesis of Carbon-12, the primary component of life and a crucial bottleneck in the synthesis of other elements. An excited Carbon-12 nuclei is formed inside stars by the fusion of 3 alpha particles into what is called the Hoyle state. Experimentally, the Hoyle state has been investigated only qualitatively but in a recent paper [2], the low energy states of Carbon-12 was calculated using computational *ab initio* methods based on first principles calculations. The development of high computing power has led to significant progress in the application of many of these methods in calculating properties of quantum systems which would otherwise be infeasible to measure. Many of these methods have the virtue of being general in their application, the basic theory holds equally for electronic structure calculations as much as it does for nuclear structure ones. However the complexity of these calculations increase exponentially even for small systems so they are mostly limited to systems with a small number of particles such as light-medium nuclei.

Here we give an introduction to canonical methods used in computational many-body physics. We first cover the basic framework of density functional theory (DFT) and configuration interaction (CI) theory. Both have been applied with great success in many fields of computational physics and chemistry and extensive literature is available. CI is used as an approach to the nuclear many-body problem in what is known as the nuclear shell model, which forms the basic framework for nuclear structure calculations. Shell model calculations can reproduce many experimental results making them reliable for predicting nuclei in conditions that are not experimentally feasible. We show an example by demonstrating a shell model calculation of an Oxygen nucleus.

We then introduce a Full CI program to compute the eigen-states, energies and wave functions of a general 1-D fermion system. Although rather limited in describing any real 3-D system such as a nucleus, it illustrates important theoretical concepts and implementation problems one might face when building more advanced programs. We test the validity of the program by analyzing the results and comparing them to analytical results when possible. We comment on the physics of the results and focus on the different effects of changing the parameters of the system such as the number of particles and range of interaction on the convergence rate of the program, the precision as well as note any emerging phenomena. We conclude with a discussion on improvements that could be made to the program and its limitations as well as its extended use in generating training data for a neural network to perform the same task.

2 Theory

We start by defining our general nuclear Hamiltonian for a N-particle system in an external potential with 2-body interaction,

$$\hat{H} = -\sum_{i=1}^{N} \tfrac{1}{2}\nabla_i^2 - \sum_{i=1}^{N} v(\mathbf{r}_i) + \sum_{i<j}^{N} U(\mathbf{r}_i, \mathbf{r}_j). \tag{2.1}$$

The first term is the kinetic 1-body operator, $v(\mathbf{r}_i)$ is the 1-body potential and $U(\mathbf{r}_i, \mathbf{r}_j)$ is the interaction between particles i and j, which is given (usually Coulomb interaction). We may write Eq.(2.1) compactly in terms of their respective operators as,

$$\hat{H} = \hat{T} + \hat{V} + \hat{U}. \tag{2.2}$$

2.1 Variational Principle

Given that the Hamiltonian $\hat{H}$ is Hermitian, its eigen-functions $|\Psi_n\rangle$ form a complete basis set. So we can write any trial wave function $|\tilde{\Psi}\rangle$ as a linear combination of $|\Psi_n\rangle$,

$$\tilde{\Psi} = c_0\Psi_0 + c_1\Psi_1 + c_2\Psi_2 + \dots. \tag{2.3}$$

Note that $|\tilde{\Psi}\rangle$ has to be normalized. Eq. (2.3) shows that $|\tilde{\Psi}\rangle$ can contain contributions from eigen-states with higher energies than the ground state $|\Psi_0\rangle$. Therefore, One can then show that the trial energy $E[\tilde{\Psi}]$ corresponding to the trial wave function, is always higher than the ground state energy E_0 [6],

$$\langle\Psi|\hat{H}|\Psi\rangle \geqslant \langle\Psi_0|\hat{H}|\Psi_0\rangle\,,\ \forall\Psi, \qquad\qquad E[\Psi] \geqslant E_0,\ \forall\Psi. \tag{2.4}$$

This is the *variational principle*. The minimization of the energy functional is equivalent to solving the time-independent Schrödinger equation. However, this gives a more practical form since minimization of the basis components reduces to a diagonalization problem. Due to its flexibility of using approximate wave functions as upper bounds to the true energy, it is one of the methods of choice for most modern many-body structure calculations and is the one used in both density functional theory and configuration interaction.

2.2 Basic Density Functional Theory

One of the most powerful modern computational method available for calculating electronic structure is called *density functional theory*. The idea has its origins in the early 1920's Thomas-Fermi model. There electrons are treated using statistical mechanics, allowing the calculation of the electron *density*, from which the ground state energy can be found [3]. Although the model was an important first step in developing a many-body theory of electronic structure, it had very limited accuracy and only gave qualitative results. DFT involves reformulating the many-body problem by uniquely describing the wave function in terms of the ground state density, instead of the external potential. This was first done in the 1960s in the framework of the two Hohenberg-Kohn theorems [4].

2.2.1 The Hohenberg–Kohn Theorems

For a N-body system described with the Hamiltonian Eq.(2.1) with a given 2-body interaction, the choice of external potential $v(\mathbf{r})$ completely determines the Hamiltonian. The first

Hohenberg-Kohn theorem states that $v(\mathbf{r})$ is completely determined, within a constant, by the *ground state density*,

$$\rho(\mathbf{r}) = N \int |\Psi(\mathbf{r}, \mathbf{r_2} \dots \mathbf{r_N})|^2 d\mathbf{r_2} \dots d\mathbf{r_N}, \tag{2.5}$$

normalized to the number of electrons in the system,

$$\int \rho(\mathbf{r}) d\mathbf{r} = N. \tag{2.6}$$

It then follows that $\rho(\mathbf{r})$ also uniquely determines the ground state energy E_0. Given this dependence, we can now rewrite the ground state energy as a functional of the density instead as,

$$E[\rho] = T[\rho] + V[\rho] + U[\rho] \tag{2.7}$$

$$= F[\rho] + \int \rho(\mathbf{r}) v(\mathbf{r}) d\mathbf{r} \tag{2.8}$$

where,

$$F[\rho] = T[\rho] + U[\rho] \qquad\qquad V[\rho] = \int \rho(\mathbf{r}) v(\mathbf{r}) d\mathbf{r}. \tag{2.9}$$

Here we introduce $F[\rho]$, which is independent of the external potential $v(\mathbf{r})$ and is exact for a given ground-state density, it is called the *universal functional* of $\rho(\mathbf{r})$. Any system that has the same form for $U[\rho]$ will also have the same $F[\rho]$. However, $F[\rho]$ is highly non-trivial and difficult to derive. This problem will be approached indirectly later using the Kohn-Sham (KS) method.

The second theorem provides an analogous variational principle Eq.(2.4) for the energy functional of a trial density $\tilde{\rho}(\mathbf{r})$, under the constraint Eq.(2.6) [3],

$$E[\tilde{\rho}] \geqslant E_0. \tag{2.10}$$

Or expressed in Lagrange multiplier form,

$$\delta\{E[\rho] - \mu[\int \rho(\mathbf{r}) d\mathbf{r} - N]\} = 0 \tag{2.11}$$

which gives the Euler-Lagrange equation,

$$\mu = \frac{\delta E[\rho]}{\delta \rho(\mathbf{r})} = v(\mathbf{r}) + \frac{\delta F[\rho]}{\delta \rho(\mathbf{r})}, \tag{2.12}$$

where the multiplier μ is the chemical potential. The above expression is the main working equation of DFT. To find an expression for the universal functional we turn to the Kohn and Sham formulation.

2.2.2 Kohn-Sham Method

The Kohn-Sham method deals with the universal functional by introducing a non-interacting reference system with the *exact* same ground state density ρ as our interacting system [5]. The Hamiltonian then consists of only 1-body operators without the 2-body interaction term,

$$\hat{H}_s = -\sum_i^N \tfrac{1}{2}\nabla^2 + \sum_i^N v_s(\mathbf{r}) = \sum_i^N h_i, \tag{2.13}$$

where the first term represents the kinetic energy $T_s[\rho]$ of our non-interacting system. This system has an exact solution in the form of a single Slater determinant wave function and it is a much easier problem to solve. It involves solving a set of N uncoupled eigen-equations,

$$\hat{h}_s\phi_i = [-\tfrac{1}{2}\nabla^2 + v_{\rm s}]\phi_i = \epsilon_i\phi_i \tag{2.14}$$

where ϕ_i are the N lowest eigen-states of the single-electron Hamiltonian $\hat{h}_s$. We can use $T_s[\rho]$ to approximate T by introducing it in the universal functional,

$$F[\rho] = T_s[\rho] + E_{xc}[\rho]. \tag{2.15}$$

Here we define the *exchange-correlation* energy E_{xc},

$$E_{xc}[\rho] = T[\rho] - T_s[\rho] + U[\rho] \tag{2.16}$$

It is the only unknown in the method and can be approximated [3]. Inserting our new expression for the universal functional into (2.12) gives,

$$\mu = v_{\rm eff}(\mathbf{r}) + \frac{\delta T_s[\rho]}{\delta\rho(\mathbf{r})}, \tag{2.17}$$

where the *KS effective potential* is defined as,

$$v_{\rm eff}(\mathbf{r}) = v(\mathbf{r}) + \frac{\delta E_{xc}[\rho]}{\delta\rho(\mathbf{r})}. \tag{2.18}$$

Eq.(2.17)-(2.18) are the Kohn-Sham equations. Notice that Eq.(2.17) has the form of Eq.(2.12) for a non-interacting system in an external potential $v_{\rm eff}(\mathbf{r})$. We can thus solve the uncoupled N-particle equations Eq.(2.14) with $v_s = v_{\rm eff}$ to obtain the orbitals needed to find the density of our original system

$$\rho(\mathbf{r}) = \sum_i^N |\phi_i(\mathbf{r})|^2. \tag{2.19}$$

2.3 Configuration Interaction

The simplest approximation to a N-electron ground state function is an anti-symmetric product of N occupied single-particles orbitals $\{\chi_i\}$, known as a Slater determinant or SD [6],

$$\Psi(\mathbf{x}_1, \mathbf{x}_2 \ldots, \mathbf{x}_N) = \frac{1}{\sqrt{N!}}\mathrm{Det}[\chi_a\chi_b\ldots\chi_k] = |ab\ldots k\rangle \tag{2.20}$$

where the orbital χ_i is denoted by i. The constant is for normalization, since the determinant produces $N!$ terms. The anti-symmetric requirement comes from the fact that the particles we will be considering are fermions. Thus, the wave function flips sign on exchange of 2 particles, which is a property of the determinant.

Given a set of K orbitals, picking the lowest N orbitals to occupy gives the ground state determinant,

$$|\Psi_0\rangle = |12\ldots ab\ldots N\rangle\,. \tag{2.21}$$

This is the starting point of the Hartree-Fock approximation, which is the best single-determinant approximation of the wave function [6]. We note here that a basis set of orbitals needs to be infinite to be complete. Since this is infeasible, we truncate the set to K orbitals. However as we will see soon, even a finite set can rapidly become infeasible for computational purposes.

The ground state determinant $|\Psi_0\rangle$ isn't the only possible determinant. Given a choice from the set of K orbitals, we can pick out any N orbitals to put our particles in. So in total we have $\binom{K}{N}$ possible determinants. All these determinants along with the ground determinant $|\Psi_0\rangle$ can be used in linear combination to produce a more accurate approximation of the ground state wave function [6]. To make things easier, we can group these determinants based on how many particles are excited into a higher orbital relative to the ground determinant. For example, a doubly excited determinant is one in which two particles have been excited from χ_a and χ_b to χ_r and χ_s, with respect to the ground state determinant $|\Psi_0\rangle$,

$$|\Psi_{ab}^{rs}\rangle = |12...r...s...N\rangle\,. \tag{2.22}$$

This can similarly be done for all N-tuply excited determinants. These determinants can also be labelled based on how many particles are excited and how many "holes" are produced, for example 2p-2h for the above determinants. We can write down the exact wave function as a linear combination of all these possible determinants,

$$|\Psi\rangle = c_0\,|\Psi_0\rangle + \sum_{ra} c_a^r\,|\Psi_a^r\rangle + \sum_{\substack{a<b\\r<s}} c_{ab}^{rs}\,|\Psi_{ab}^{rs}\rangle + \sum_{\substack{a<b<c\\r<s<t}} c_{abc}^{rst}\,|\Psi_{abc}^{rst}\rangle + \dots \tag{2.23}$$

It can be shown that this set of determinants $\{\Psi_i\}$ also form a complete basis set for any N-electron wave function. This stems from the fact that the determinants themselves are made of the complete set of orbitals $\{\chi_i\}$. We can now rewrite our Hamiltonian in terms of this basis. We evaluate the matrix elements by splitting the Hamiltonian into 1-body and 2-body operators,

$$\langle\Psi_i|\,\hat{H}\,|\Psi_j\rangle = \langle\Psi_i|\,\hat{h}\,|\Psi_j\rangle + \langle\Psi_i|\,\hat{U}\,|\Psi_j\rangle\,. \tag{2.24}$$

The matrix elements are calculated using second quantization (Appendix A),

$$\langle\Psi_n|\,\hat{h}\,|\Psi_m\rangle = \sum_{ij}\langle i|\,h\,|j\rangle\,\langle\Psi_n|\,a_i^\dagger a_j\,|\Psi_m\rangle \tag{2.25}$$

$$\langle\Psi_n|\,\hat{U}\,|\Psi_m\rangle = \sum_{ijkl}\langle ij|\,U\,|kl\rangle\,\langle\Psi_n|\,a_l^\dagger a_i^\dagger a_k a_j\,|\Psi_m\rangle\,, \tag{2.26}$$

where the 2-body integral term is,

$$\langle ij|\,U\,|kl\rangle = \int \chi_i(x_1)\chi_j(x_2)U(x_1,x_2)\chi_k(x_1)\chi_l(x_2)dx_1dx_2. \tag{2.27}$$

As discussed in Appendix A, the majority of these groupings get cancelled out in the Hamiltonian, making it a *sparse* matrix. Diagonalizing the Hamiltonian gives us the approximate ground-state eigen-energy E_0. This method is known as Configuration-Interaction [6]. If all possible SDs in a finite orbital basis are used in the calculation then it is called Full Configuration-Interaction or *Full CI*, which is the best possible approximation to the true wave function given a finite single-particle orbital set. However practically, it becomes very computationally intensive even for a few particle system due to the combinatorial growth of the number of SDs required. In practice, not all determinants are calculated since only a few determinants have any meaningful contribution to the final diagonalization of the Hamiltonian.

3 Nuclear Shell Model Example

CI is used as an approach to the nuclear many-body problem in what is known as the *shell model*. In traditional shell model, the many body system is approximated to independent particles stacked in shells in the presence of a central potential [7]. An important of application of CI is the valence space nuclear shell model [1]. The nuclear shell model is used to describe a variety of properties of nuclei. In this model, it is often assumed that the presence of an inert core. In addition to this, N nucleons are added and are allowed to interact within a limited space with an effective Hamiltonian. This limited space is called the valence space and the neutrons added on the core are called valence neutrons. In this work, full CI was done on an inert Oxygen-16 nucleus core, in addition of which N valence neutrons were added in the valence space $1d_{5/2}$-$2s$ (shown in Figure 1) comprising 12 orbitals.

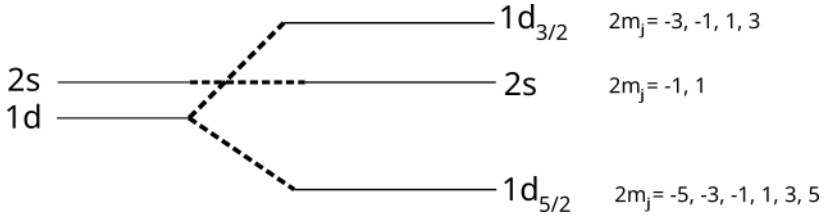

Figure 1: Energy levels of the first 12 valence orbitals of O_{16}

The basis used for the orbitals in this example are the 3-D harmonic oscillator basis functions. The matrix elements of the effective Hamiltonian were taken from USDB Hamiltonian data [9]. All possible determinants were generated by simple combinatorics, with the restriction that the orbitals in each determinant couple in the subspace with a given angular momentum M. The constructed Hamiltonian was then diagonalized to obtain the eigen-functions and energies. Fig. 2 shows an example calculation of the ground state.

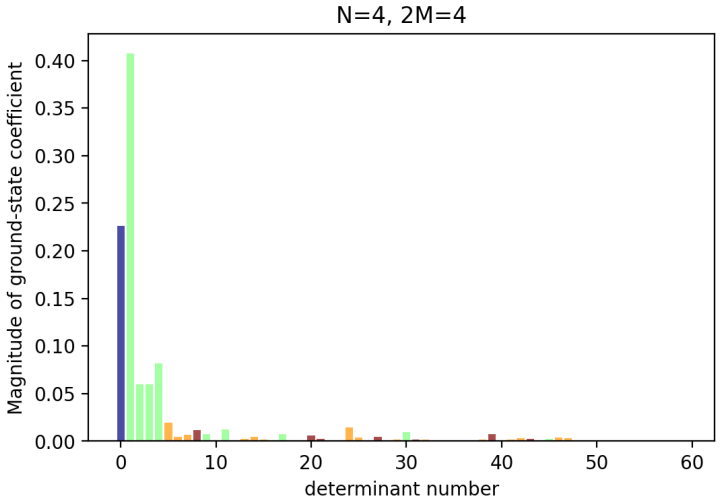

Figure 2: Distribution of ground-state weights for each determinant with 4 particles and 2M = 4, where M is the sum of the angular momentum of the particles. Here, the SDs are sorted in increasing order of each SD's summed single-particle orbital energies and are grouped based on their excitation (Blue is the ground determinant, Green are the 2p-2h determinants, Orange are 3p-3h, etc.).

Note that in this case, there is no contribution from 1p-1h determinants because exciting just one particle from a determinant with angular momentum M cannot produce another determinant with the same angular momentum.

4 Full 1-D Configuration Interaction

Here we demonstrate a Full CI program to model a 1-D quantum system. This was done in Python from scratch, with the previous 3-D code used as example.

4.1 Code

The manipulation and storage of SDs was done in bit representation [10], where the occupation of a single-particle state is denoted by either a 1 or 0. For example, for a set of 5 orbitals, the SD $|13\rangle$ is represented by 10100 (or 20 in decimal representation). This forms a convenient framework for creation and destruction operators which can also be represented in binary form,. For example, a_3 and $a_3^\dagger$ can be represented as 00100. Note that whether the binary operator is destructive or constructive depends on the whether that state is occupied in the SD it acts on. The actual operation is done by taking the XOR between the operator and the SD. The XOR of 2 bits gives 1 only when one of the bits is 1 (or only when both bits are different). As an example, the destruction operator a_3 acting on the above SD can be found by taking the XOR of their respective bit representations.

$$a_3 |13\rangle = |3\rangle \oplus |13\rangle = (00100) \oplus (10100) = (10000) = |1\rangle . \tag{4.28}$$

If the above was interpreted as a creation operator instead, it would produce an invalid result. It is important in implementation to guarantee that the correct operator is chosen based on the state occupation of the SD. Bit representation also allows for more efficient manipulation of SDs since each SD and operators can now be stored like an integer.

For the single-particle basis, the Hermite functions of the 1-D harmonic oscillator were used with $\hbar = \omega = 1$. All possible SDs are generated and sorted by the sum of occupied single-particle state energies of each SD. We used 4 potentials. 2 harmonic potentials,

$$V_H(x) = \frac{1}{2} m x^2 \tag{4.29}$$

with $m = 1$ and $m = 2$, the latter being narrower. A Woods-Saxon potential, which is a mean field radial potential used to model the total mean interaction of all the nucleons in a nucleus. It is used in the nuclear shell model and is of great importance in nuclear structure theory which is the main field of focus for this code. We use this potential to test the generalization of the code but also to use something similar in shape to the harmonic potential to better understand the gradual change in the convergence rate of the program. It takes the form,

$$V_{WS}(x) = -\frac{V_0}{1 + \exp\left(\frac{x-R}{a}\right)} \tag{4.30}$$

where the chosen parameters for the tests were $V_0 = 10$, $a = 0.2$ and $R = 3.4$. These were chosen so the potential looks similar to a harmonic potential. We also use a corrugated Woods-Saxon, which just includes a superimposed sine wave,

$$V_{WSC}(x) = V_{WS}(x) + \sin x. \tag{4.31}$$

For the generation of the matrix elements, a Gaussian 2-body interaction was used,

$$U(x_1, x_2) = \frac{1}{\sqrt{a\pi}} \exp\left(-\frac{(x_2 - x_1)^2}{a} \right) \tag{4.32}$$

of different widths a. The interaction is normalized to keep it's strength constant while changing the range (i.e the width). This is important when it comes to the integration of the 2-body matrix elements. A Gaussian was used since it is flexible and has been used in physical interactions and makes integration of the elements easier [11].

For the integrals, suitable bounds and tolerance were chosen for a balance between acceptable precision and generation time and only calculated if the integrand was of even parity, since symmetric integration of an odd function vanishes. The calculation of the matrix elements took a substantial amount of time with increase in the number of basis states used, so the elements were stored when generated and read off when needed.

4.2 Testing and Results

To verify the code's validity, we run some test cases. As measure for convergency, we will use the error between the produced eigen-energies from diagonalizing the Hamiltonian for different number of basis states and true values for the eigen-energies, which is taken as the eigen-energies for the highest number of basis states, or analytical values if possible. The error will be plotted for the ground-state and the first 4 excited states. We also plot the coefficient of each SD in the final diagonalization for the ground until 3rd excited state, we call this the "Slater profile". The SDs are sorted in increasing order of their sum of single-particle basis energy sum.

For most of the tests with 2-body interaction, due to limitations in computational power, only elements from up to ≈ 12 basis states were calculated. This produced ≈ 1569 non-zero 2-body elements. There was no real computational limitations on the 1-body part where ≈ 130 basis states were used, totalling 4160 non-zero 1-body elements.

4.2.1 Only 1-body elements

We first test the code with only 1 particle in different 1-body potentials. Thus, only 1-body elements are used.

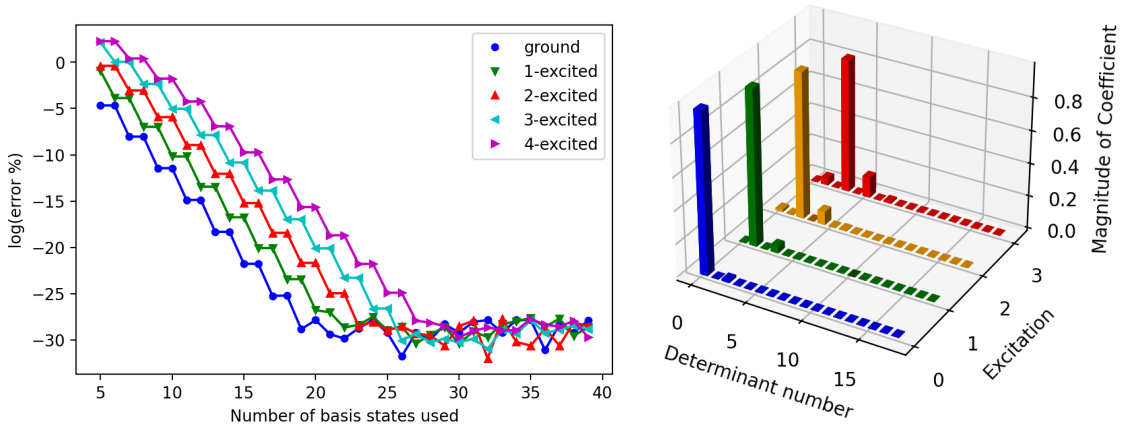

Figure 3: Error plot of the ground and excited states against number of states used (left) expressed in $\log_{10}$ of the percentage. Slater profile of the calculation for the different excitations as in Fig. 2 (right) for 1 particle in a harmonic potential with $m = 2$. Error was calculated relative to the analytical eigenvalues for the harmonic oscillator: $(n + \frac{1}{2})h\omega$

In Fig. 3, we compare the calculations of the system with Harmonic potential in Eq.(4.29) with $m = 2$. The calculation was done using basis states from Harmonic Oscillator eigen-state

calculated with $m = 1$. The energy is compared to the analytical eigen-energies to obtain the results. The calculated energies converge as more basis states are used to generate the matrix elements, with more excited states requiring more basis states than lower ones. Note the step-like pattern. Since the ground eigen-state is of even parity, only even basis state contribute to improving the approximation of the energy as seen in the step-like dips. The 1-excited eigen-state is odd, so the error dips on the odd states instead and so forth. The noise after around 25 states is due to the double precision limit reached by the code.

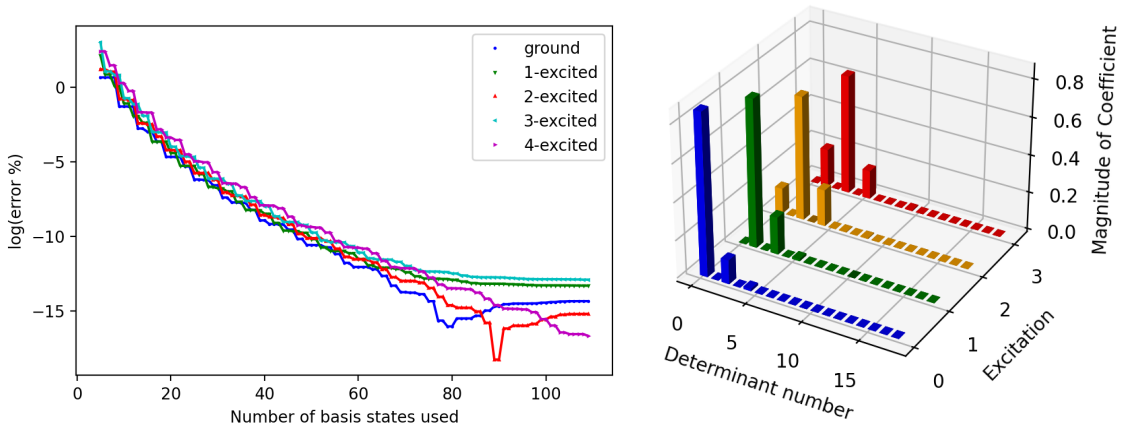

Figure 4: Error plot of the ground and excited states against number of states used (left) expressed in $\log_{10}$ of the percentage. Slater profile of the calculation for the different excitations as in Fig. 2 (right) for 1 particle in a Woods-Saxon potential. Error was calculated relative to the eigen-energies produced with 140 states

In Fig. 4, we calculate the 1-particle system with Woods-Saxon potential using the same basis states as previously. The error was calculated compared to eigenvalues calculated using 140 basis states. There is much slower convergence for the Woods-Saxon potential compared to that of the harmonic potential with $m = 2$ since the latter is closer in shape to that of the basis potential, so it requires less basis states to approximate its own eigenfunctions. The Woods-Saxon potential eigen-states contain contributions from both even and odd basis states. This is also why the Slater profile is not as concentrated.

4.2.2 1-body + 2-body elements

We now introduce a second particle as well as 2-body Gaussian interaction as in Eq. (4.32).

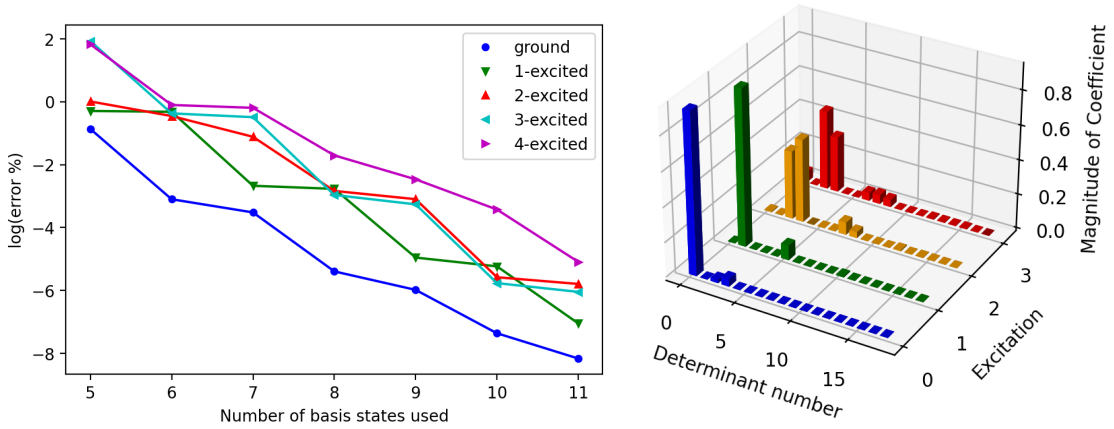

Figure 5: Error plot of the ground and excited states against number of states used (left) expressed in $\log_{10}$ of the percentage. Slater profile of the calculation for the different excitations as in Fig. 2 (right) for 2 particles in a harmonic potential with $m = 2$. A Gaussian with $a = 1$ was used for the 2-body interaction. Error was calculated relative to eigen-energies produced with 13 basis states.

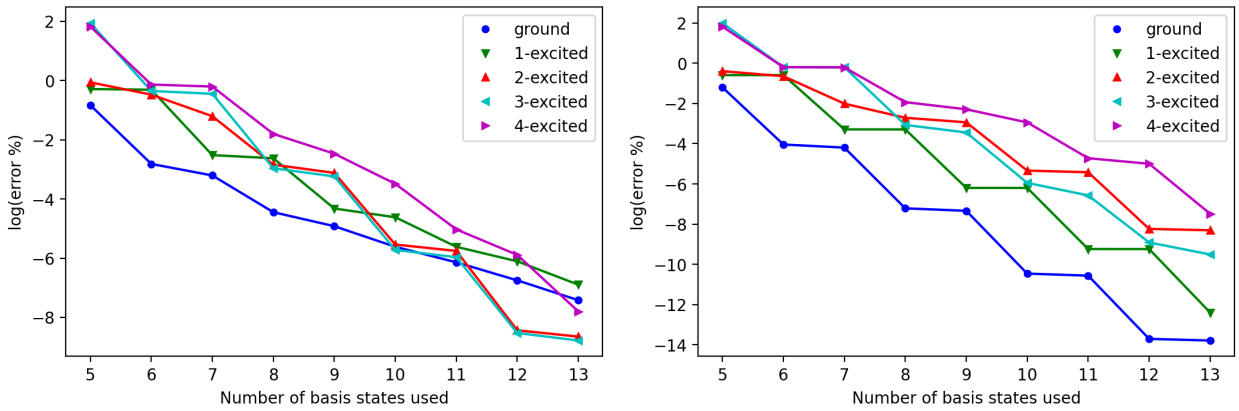

Figure 6: Error plot of the ground and excited states against number of states used for 2 particles in harmonic potential with $m = 2$. A Gaussian with $a = 0.5$ (left) and $a = 10$ (right) was used for the 2-body interaction. Error was calculated relative to eigen-energies produced with 15 states

In Fig. 5 and Fig. 6, we calculate a system of 2 particles in a harmonic potential Eq.(4.20) and Gaussian interaction Eq.(4.31) with different widths. The error was calculated with respect to the calculation with N states. A wider Gaussian interaction gives a faster and more uniform convergence. The effect of changing the width of the interaction on the convergence rate can be investigated using Heisenberg's uncertainty principle. For a narrow Gaussian interaction, taking the Fourier transform into momentum space gives a wide Gaussian. This means particles with a greater range of momenta, energies, are allowed to interact, which produces bigger coupling of states, giving a slower convergence. For a wide Gaussian interaction instead, the transformed Gaussian will cover a narrow range of momenta. Particles then only interact with other particles of similar energies, which gives a faster convergence. In the case of an infinitely wide Gaussian interaction, which is just a constant, the transform is a Dirac delta function and the particles

only interact with other particles of the exact same energy. This effectively gives no 2-body interaction terms. This can also be seen in first quantization where the 2-body integral terms (2.27) for a constant interaction are

$$\langle ij|\, V\, |kl\rangle = V \int \chi_i(x_1)\chi_j(x_2)\chi_k(x_1)\chi_l(x_2)dx_1dx_2 = V\delta_{ik}\delta_{jl} \tag{4.33}$$

where V is a constant. These terms are non-zero only on the diagonal and are the same value. The effect can also be seen in the Slater profiles.

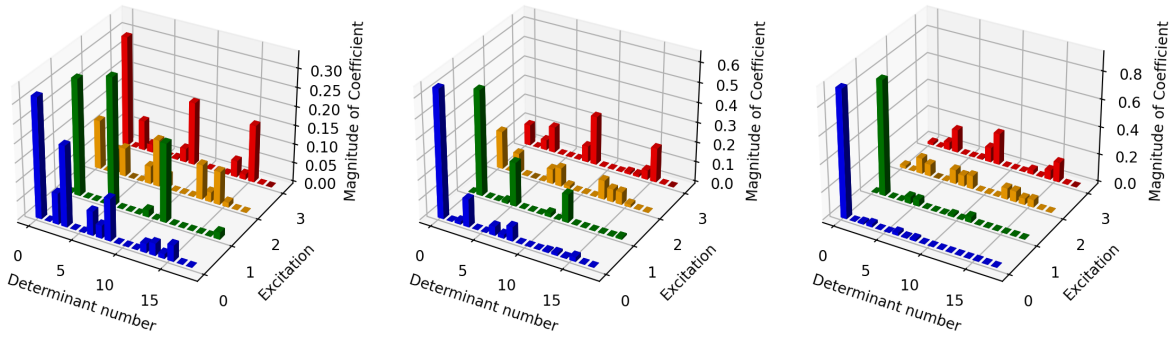

Figure 7: Slater Profile of a 2-body Corrugated Woods-Saxon potential calculation with Gaussian interaction width $a = 1$ for ground and 1st excited state for different strength interactions x1 (left), x10 (center) and x20 (right).

If we instead keep our Gaussian interaction width constant and change the interaction strength, the same effect is seen in Fig. 7. The Slater profile of a 2-body Corrugated Woods-Saxon becomes more concentrated at the ground SD with increased interaction strength. The reasoning is similar to that above in that the particles cluster due to the stronger force, reducing the spread of the Slater profile and thus increasing the convergence rate. Similar results are seen when we increase the number of particles.

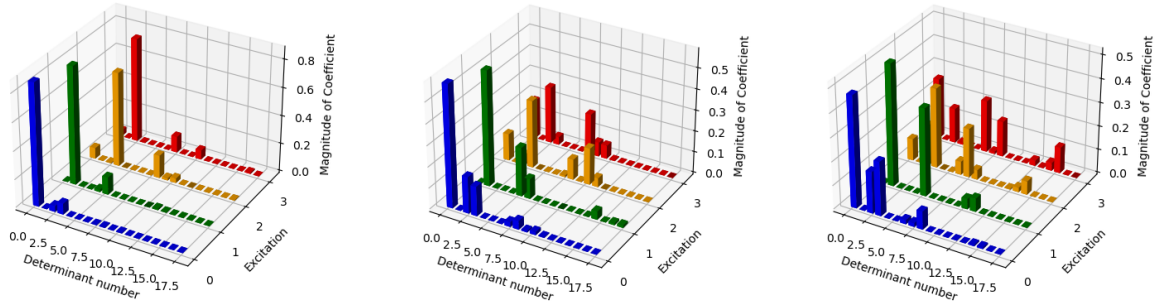

Figure 8: Slater Profile of a N-body harmonic potential with $m = 2$ calculation with $N = 3$ (left), $N = 6$ (center) and $N = 11$ (right).

The Profiles become more spread out when there are more particles initially, but the same behaviour occurs when we change the interaction strength and width.

4.2.3 1-particle Wave function

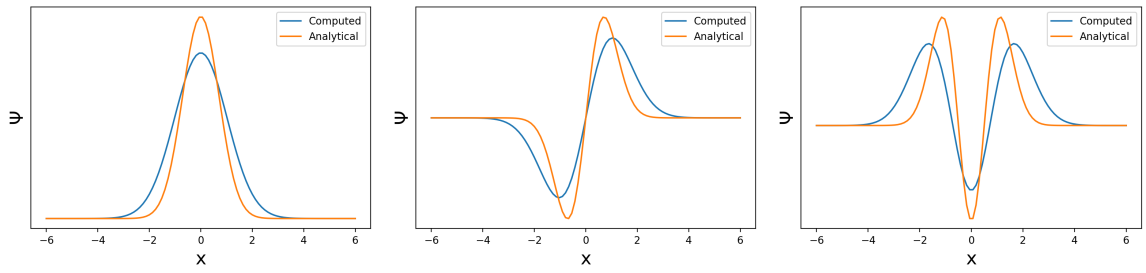

Figure 9: Ground, 1st and 2nd excited eigen-state wave functions of a harmonic potential with $m = 2$ produced from the calculation (Blue) compared to the analytical form (Orange).

We also check the validity of the produced 1-particle wave functions in Fig. 8 by comparing them to the analytical functions in the case of a harmonic potential. The precision of the results may be due the fact that the Slater profile is not as spread out, as the potential is similar to the basis potential, but the $m = 2$ potential is localizing more with respect to $m = 1$ basis with a poor representation of tails. The tail of the harmonic oscillator wave functions are exponentially decaying with a rate depended on the width of the potential. Therefore, one needs an infinite number of components to reproduce the tail with a basis of a different width. The precision could drop further if this was done for a Woods-Saxon potential instead. Note that relatively, the calculated eigen-energies are more precise than the calculated wave-functions relative to their respective references, so more states are needed to get a better approximation to the wave-functions. This is an example of the fact that in a full CI calculation, not all observables will converge at the same rate.

4.2.4 2-particle Density function

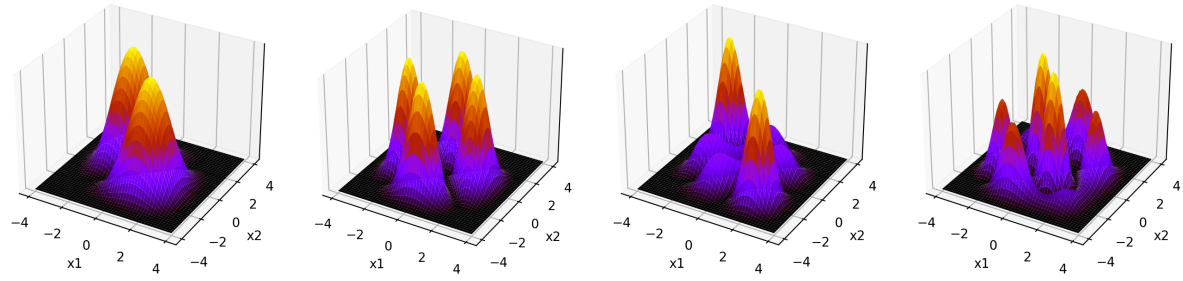

Figure 10: Density plots of ground, 1st, 2nd and 3rd excited state for a Woods-Saxon potential (left to right respectively).

In the case of 2 particles in Fig. 9, we plot the density instead defined as,

$$\rho(x_1, x_2) = |\Psi(x_1, x_2)|^2.$$

The effect of interaction strength can also be seen in the densities in Fig. 10. Note once again the increasing concentration of the state, all forms of the data presented so far point to condensation phenomena for high enough interaction strength.

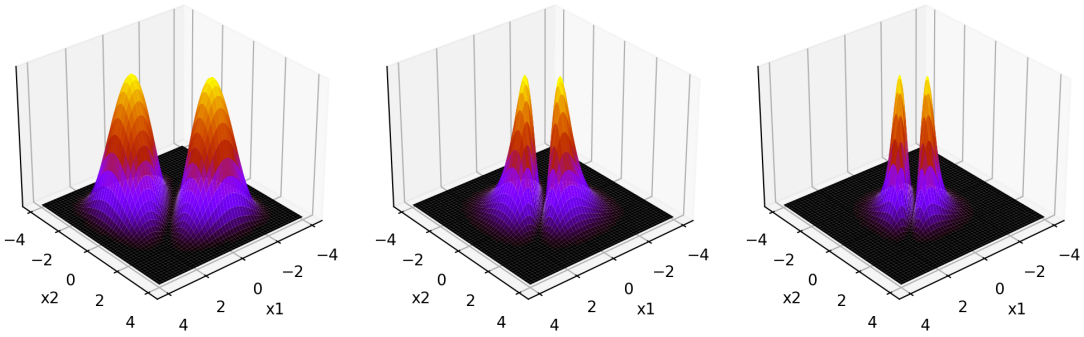

Figure 11: Density plots of ground state for a Woods-Saxon potential with different strength interactions x1 (left), x10 (center) and x100 (right).

Once the elements were calculated, the time taken for the actual construction and diagonalization of the Hamiltonian was negligible in comparison to the computation time of the elements. The numerical work was not done in coordinate space, so there were no boundary conditions and the density plots approach zero fast enough to easily define plot limits.

5 Conclusion

In this thesis work, we introduced DFT and CI formalism and used the latter to develop a general 1-D full CI program, which produced reasonable results when tested with a few potentials and provided insight into the physics of such a system as well as on how to approach developing more advanced programs to overcome limitations encountered here.

The main bottleneck in the generation of matrix elements were the 2-body integrals. This was because a general double integration algorithm was used, which is not efficient for a large number of integrations. Because of this, very few basis states were used in testing the 2-body component of the program. The integrands involved are orthogonal polynomials for which there exists more efficient integration algorithms. In our case, analytical solutions could have been used for evaluating integrals of Hermite functions and Gaussians. Such an implementation would improve the program and increase the capabilities of the possible calculations, particularly for the 2-body calculations.

The purpose of creating a functioning Full CI program was to produce data that would have been used in an attempt to train a neural network to perform the same task, but more efficiently. The data would have consisted of input-output pairs of a generated potential and its respective unique density, which is guaranteed by the Hohenberg-Kohn theorems. This unique correspondence is what could allow a trained network to generalize to any given potential. Although the 1-D quantum system modelled here is very limited in describing real-world cases, the proof of concept holds for 3-D systems when the theory and implementation is extended to include angular momentum. Therefore, Full CI is an interesting method to study many-body systems and the code developed here, rewritten perhaps in a faster language like C++ or Fortran, can be an insightful tool in study of ideal systems and methods. However the computational complexity of the calculation increases exponentially which limits this method to small systems.

A Second Quantization Formalism

Due to the indistinguishable nature of identical particles like fermions and bosons, it is useful to reformulate our mathematical model of quantum mechanics in terms of purely occupational representations of our wave functions, rather than permutation based manipulation. This approach is know as second quantization [6].

We define the annihilation operator and derive its adjoint creation operator which remove and add a particle from an orbital respectively,

$$a_i \left|ij\dots l\right\rangle = \left|jk\dots l\right\rangle, \qquad a_i^\dagger \left|jk\dots l\right\rangle = \left|ij\dots l\right\rangle, \qquad (a_i^\dagger)^\dagger = a_i. \tag{A.34}$$

If we attempt to create a particle in an orbital which is already occupied, or to remove a particle in an otherwise empty orbital, we quench the state and get 0. We also include the anti-symmetry principle on exchange of particles,

$$\left|\dots ij\dots\right\rangle = -\left|\dots ji\dots\right\rangle. \tag{A.35}$$

We can also derive the following anti-commutation relations,

$$\{a_i, a_j\} = \{a_i^\dagger, a_j^\dagger\} = 0, \qquad \{a_i^\dagger, a_j\} = \delta_{ij}. \tag{A.36}$$

Note that these relations incorporate the Pauli exclusion principle and avoid the explicit use of SDs. This also greatly simplifies varying the number of particles in the system. We define the vacuum state,

$$a_i \left|0\right\rangle = 0, \ \forall i, \tag{A.37}$$

where we construct anti-symmetric states by application of creation operators,

$$\left|12\dots N\right\rangle = a_1^\dagger \dots a_N^\dagger \left|0\right\rangle. \tag{A.38}$$

The expressions for one-body and two-body operators $\hat{O}_1$ and $\hat{O}_2$ are,

$$\hat{O}_1 = \sum_{ij} O_{ij} a_i^\dagger a_j, \qquad \hat{O}_2 = \sum_{ijkl} O_{ijkl} a_i^\dagger a_j^\dagger a_l a_k. \tag{A.39}$$

Here, O_{ij} and O_{ijkl} are just numbers representing the value of the matrix element. These can be used to easily compute matrix elements of an operator. For example, applying the 1-body operator to calculate the ground state determinant gives,

$$\left\langle\Psi_0\right| \hat{O} \left|\Psi_0\right\rangle = \sum_{ij} O_{ij} \left\langle\Psi_0\right| a_i^\dagger a_j \left|\Psi_0\right\rangle. \tag{A.40}$$

For the element to be non-zero, then by (A.34), $\{i, j\}$ must be in $\left|\Psi_0\right\rangle$. If $i \neq j$, then the element is an inner product of two different (and hence orthogonal) determinants, which is 0. The only solution is when $i = j$ where the inner product gives 1 by normalization. This simplifies the whole sum,

$$\left\langle\Psi_0\right| \hat{O} \left|\Psi_0\right\rangle = \sum_i O_{ii}. \tag{A.41}$$

The same reasoning of simplification to determinants with only certain orbitals and orthonormality of the determinant set can be also be applied to the 2-body operator and generalized to any 2 determinants used in the inner product. In fact, for any 2 determinants differing by 2 or more orbitals, the 1-body element will always be 0. If they differ by 4 or more orbitals instead, the 2-body element will always be zero [6]. Hence for a Hamiltonian in a determinant basis (for example the one used in CI) will form a sparse matrix with non-zero elements concentrated near the diagonal.

References

[1] E. Caurier, et al. "The Shell Model as Unified View of Nuclear Structure" Rev. Mod. Phys. 77 (2005), 427

[2] Evgeny Epelbaum et al., "*Ab Initio* Calculation of the Hoyle State," Phys. Rev. 106 (2011), 192501

[3] Robert G. Parr and Yang Weitao. *Density-Functional Theory of Atoms and Molecules.* Oxford University Press USA (1994)

[4] P. Hohenberg and W. Kohn "Inhomogeneous Electron Gas" Phys. Rev. 136 (1964), B864

[5] W. Kohn and L. J. Sham, "Self-Consistent Equations Including Exchange and Correlation Effects" Phys. Rev. 140 (1965), A1133

[6] Attila Szabo and Neil S. Ostlund *Modern Quantum Chemistry: Introduction to Advanced Electronic Structure Theory* Dover Publications; Revised edition (1996)

[7] L. Coraggio, et al. "Shell-model calculations and realistic effective interactions" Prog. Part. Nucl. Phys. 62 (2009), 135-182

[8] J. Dechargé and D. Gogny, "Hartree-Fock-Bogolyubov calculations with the D1 effective interaction on spherical nuclei", Phys. Rev. C 21 (1980), 1568

[9] W. A. Richter, S. Mkhize, and B. Alex Brown *sd-shell observables for the USDA and USDB Hamiltonians* Phys. Rev. C 78 (2008), 064302

[10] `https://nucleartalent.github.io/NuclearStructure/doc/pub/projects/html/projects-reveal.html`

[11] I. Reichstein and Y. C. Tang *Study of N+α system with the resonating-group method*, Nucl. Phys. A 158 (1970), 529